Dynamics of Photoinduced Charge Separation and Charge Recombination in Synthetic DNA Hairpins with Stilbenedicarboxamide Linkers

Frederick D. Lewis,* Taifeng Wu, Xiaoyang Liu, Robert L. Letsinger, Scott R. Greenfield, Scott E. Miller, and Michael R. Wasielewski*

Contribution from the Department of Chemistry, Northwestern University, Evanston, Illinois 60208

Received October 14, 1999

Abstract: The dynamics of photoinduced charge separation and charge recombination in synthetic DNA hairpins have been investigated by means of femtosecond and nanosecond transient spectroscopy. The hairpins consist of a stilbene linker connecting two complementary 6-mer or 7-mer oligonucleotide strands. Base pairing between these strands results in formation of hairpins in which the stilbene is approximately parallel to the adjacent base pair. The singlet stilbene is selectively quenched by guanine, but not by the other nucleobases, via an electron-transfer mechanism in which the stilbene singlet state is the electron acceptor and guanine is the electron donor. In a hairpin containing only A:T base pairs, no quenching occurs and the restricted geometry results in a long stilbene lifetime and high fluorescence quantum yield. In families of hairpins which contain a single G:C base pair at varying locations in the hairpin stem, the stilbene fluorescence lifetime and quantum yield decrease as the stilbene−guanine distance decreases. Transient absorption spectroscopy is used to monitor the disappearance of the stilbene singlet and the formation and decay of the stilbene anion radical. Analysis of these data provides the rate constants for charge separation and charge recombination. Both processes show an exponential decrease in rate constant with increasing stilbene−guanine distance. Thus, electron transfer is concluded to occur via a single-step superexchange mechanism with a distance dependence $\beta = 0.7$ Å^{-1} for charge separation and 0.9 Å^{-1} for charge recombination. The rate constants for charge separation and charge recombination via polyA vs polyT strands are remarkably similar, slightly larger values being observed for polyA strands. The dynamics of electron transfer in hairpins containing two adjacent G:C base pairs have also been investigated. When the guanines are in different strands, the second guanine has little effect on the efficiency or dynamics of electron transfer. However, when the guanines are in the same strand, somewhat faster charge separation and slower charge recombination are observed than in the case of hairpins with a single G:C base pair. Thus, the GG step functions as a shallow hole trap. The relationship of these results to other theoretical and experimental studies of electron transfer in DNA is discussed.

Introduction

The structure and properties of duplex DNA have a special fascination for chemists, materials scientists, and life scientists.[1,2] The possibility that the one-dimensional array of π-stacked base pairs in B-form DNA might serve as a pathway for charge migration was suggested over 30 years ago.[3] Interest in DNA electron transfer has been spurred by its relevance to oxidative damage and repair mechanisms in DNA[4] and by its potential applications in molecular electronics.[5] Recent experimental and theoretical investigations of photoinduced electron transfer in DNA have provided support for the operation of two distinct mechanisms: a single-step superexchange mechanism and a multistep hole-hopping mechanism.[6,7] In addition to mechanisms that are consistent with modern theories of electron transfer, it has been proposed that an ultrafast photoinduced electron-transfer process involving intercalated donors and acceptors can occur with little or no distance dependence.[8] According to this paradigm, duplex DNA can function as a "molecular wire" or "π-way".[9]

The superexchange mechanism treats the π-stacked base pairs separating the primary electron donor and acceptor (D and A) as a bridge (B) which contributes one or more delocalized virtual electronic states.[10,11] According to eq 1, a simplified form of the Marcus−Levich−Jortner equation for nonadiabatic electron

* Address correspondence to either author. E-mail: lewis@chem.nwu.edu or wasielew@chem.nwu.edu.

(1) *Bioorganic Chemistry: Nucleic Acids*; Hecht, S. M., Ed.; Oxford University Press: Oxford, 1996.

(2) (a) Winfree, E.; Liu, F.; Wenzler, L. A.; Seeman, N. C. *Nature* **1998**, *394*, 539−544. (b) Storhoff, J. J.; Mirkin, C. A. *Chem. Rev.* **1999**, *99*, 1849−1862.

(3) Eley, D. D.; Spivey, D. I. *Trans. Faraday Soc.* **1962**, *58*, 411−415.

(4) Armitage, B. *Chem. Rev.* **1998**, *98*, 1171−1200.

(5) (a) Mirkin, C. A.; Ratner, M. A. *Annu. Rev. Phys. Chem.* **1992**, *43*, 719−754. (b) Tour, J. M. *Chem. Rev.* **1996**, *96*, 537−553. (c) de Silva, A. P.; Gunaratne, H. Q. N.; Gunnlaugsson, T.; Huxley, A. J. M.; McCoy, C. P.; Rademacher, J. T.; Rice, T. E. *Chem. Rev.* **1997**, *97*, 1515−1566. (d) Willner, I. *Acc. Chem. Res.* **1997**, *30*, 347−356. (e) Fox, M. A. *Acc. Chem. Res.* **1999**, *32*, 201−207.

(6) For recent commentaries see: (a) Wilson, E. K. *Chem. Eng. News* **1998**, *76* (30), 51−54. (b) Wilson, E. K. *Chem. Eng. News* **1999**, *77* (34), 43−48. (c) Wu, C. *Sci. News* **1999**, *156*, 104−106. (d) Ratner, M. *Nature* **1999**, *397*, 480−481.

(7) For recent reviews see: (a) Holmlin, R. E.; Dandliker, P. J.; Barton, J. K. *Angew. Chem., Int. Ed. Engl.* **1997**, *36*, 2714−2730. (b) Netzel, T. L. In *Organic and Inorganic Photochemistry Vol 2*.; Ramamurthy, V., Schanze, K. S., Eds.; Dekker: New York, 1998; pp 1−54. (c) Barbara, P. F.; Olson, E. J. C. *Adv. Chem. Phys.* **1999**, *107*, 647−676.

(8) (a) Murphy, C. J.; Arkin, M. R.; Ghatlia, N. D.; Bossmann, S.; Turro, N. J.; Barton, J. K. *Proc. Natl. Acad. Sci. U.S.A.* **1994**, *91*, 5315−5319. (b) Arkin, M. R.; Stemp, E. D. A.; Holmlin, R. E.; Barton, J. K.; Hörmann, A.; Olson, E. J. C.; Barbara, P. F. *Science* **1996**, *273*, 475−479.

(9) Turro, N. J.; Barton, J. K. *J. Biol. Inorg. Chem.* **1998**, *3*, 201−209.

10.1021/ja993689k CCC: $19.00
Published on Web 03/14/2000

$$k_{cs} = k_o e^{-\beta R} \quad (1)$$

transfer, the rate constant for charge separation, k_{cs}, in a D−B−A system is dependent upon a preexponential factor k_o, the D−A center-to-center distance R, and an exponential parameter β, which is dependent upon the nature of the bridge and its coupling with D and A. Values of β for electron transfer in proteins and most model D−B−A systems lie in the range 1.0−1.4 Å^{-1};[12] however, smaller values are observed for bridges with conjugated π-orbitals, and an example of wire-like behavior in a D−B−A system has recently been reported by Wasielewski et al.[13] Values of β reported for DNA range from 1.4 to <0.1 Å^{-1};[6] however, values toward the low end of this range may be indicative of a different mechanism for electron transfer, in which case the use of β to define the slope is not appropriate. The occurrence of hole hopping in DNA has been investigated by Barton,[14] Giese,[15] and Schuster[16] and their co-workers. According to eq 2, the rate constant for hole hopping, k_{hop},

$$k_{hop} = PN^{-\eta} \quad (2)$$

should depend on the number of hopping steps, N, and the exponent η, which has a value between 1 and 2. Schuster et al.[16b] report a slope of 0.017 Å^{-1} for a plot of ln(k_{hop}) vs D−A separation.

Experimental studies of distance-dependent photoinduced electron transfer in DNA have employed several different systems and methodologies.[6,7] The initial studies of Barton and Turro[8] employed randomly intercalated metal complexes as excited acceptors and either a second intercalator, nucleobase, or modified nucleobase as the donor. Uncertainty concerning the donor−acceptor separation has made the interpretation of these studies problematic; however, the recent studies of Harriman[17] provide a value of $\beta = 1.0$ A^{-1}, which is independent of the base-pair sequence. A more precise definition of the D−A distance is made possible by the use of oligonucleotide conjugates which possess a covalently attached probe chromophore. In the first such study, Meade and Kayyem[18] found that the rate constant for electron transfer between two nonintercalated octahedral ruthenium complexes attached to opposite ends of an eight-base-pair duplex was similar to that for a protein bridge. Stronger coupling of the duplex bridge with D and A requires the use of planar chromophores which are π-stacked with the duplex. This has been accomplished in several ways. Barton and co-workers[19,20] have employed several different chromophores tethered to the end of an oligonucleotide, which are proposed to intercalate between base pairs near the end of the duplex. Fukui and Tanaka[21] employed DNA−acridine conjugates in which the acridine is proposed to substitute for a base pair upon hybridization with a complementary oligonucleotide. Both end-tethered and mid-strand-tethered anthraquinone chromophores have been employed by Schuster and co-workers.[16] The former are proposed to form a π-stacked complex with the terminal base pair and the latter to intercalate adjacent to the point of attachment. Recently, Kelly and Barton[22] have investigated the interaction of fluorescent nucleobase analogues of adenine with donor nucleobases. A fundamentally different approach has been employed by Giese and co-workers,[15] who have employed a photocleavage reaction to irreversibly generate a guanine cation radical which can undergo hole transfer to a trap site consisting of three guanines in the same strand (a GGG step).

In most studies reported to date, relative yields of luminescence quenching or strand cleavage have been determined as a function of D−A separation and assumed to be proportional to relative rates of electron transfer. Whereas such studies are indicative of the occurrence of long-distance electron transfer in DNA, they fail to provide direct evidence for the formation and decay of radical ion intermediates, nor do they provide information about the efficiency or dynamics of electron transfer. In cases where absolute quantum yields for either luminescence or cleavage have been reported, they are often very small, raising the question as to whether they are representative of the behavior of the average DNA duplex structure or represent pathways of low probability. Measurement of the decay times of the probe chromophore by time-resolved fluorescence or transient absorption spectroscopy provides kinetic data which can be interpreted in terms of an electron-transfer quenching model. However, interpretation can be complicated when, as is generally the case, multiple decays are encountered. Transient absorption spectroscopy can also be used to directly observe the formation and decay of the radical ion intermediates in photoinduced electron-transfer processes as well as the decay of the initial excited state. Such measurements have been routinely employed to determine the kinetics of charge separation and charge recombination in synthetic D−B−A systems and in proteins and also aid in the assignment of multiple decay components to specific species.[12,13] No matter what the spectroscopic method employed, an electron-transfer mechanism cannot be firmly established without the direct observation of one or both products of electron transfer.

Our approach to the investigation of distance-dependent electron transfer in DNA is based on the use of hairpin-forming (bis)oligonucleotide conjugates in which an organic or metal complex chromophore serves as a linker between two complementary oligonucleotide arms.[23−25] This approach was suggested by the observation of Letsinger and Wu[26] that hairpins with a stilbenedicarboxamide linker and polyT−polyA stems are strongly fluorescent but that hairpins with polyG−polyC stems

(10) Jortner, J.; Bixon, M.; Langenbacher, T.; Michel-Beyerle, M. E. *Proc. Natl. Acad. Sci. U.S.A.* **1998**, *95*, 12759−12765.

(11) (a) Risser, S. M.; Beratan, D. N.; Meade, T. J. *J. Am. Chem. Soc.* **1993**, *115*, 2508−2510. (b) Priyadarshy, S.; Risser, S. M.; Beratan, D. N. *J. Phys. Chem.* **1996**, *100*, 17678−17682. (c) Beratan, D. N.; Priyadarshy, S.; Risser, S. M. *Chem. Biol.* **1997**, *4*, 3−8. (d) Priyadarshy, S.; Risser, S. M.; Beratan, D. N. *J. Biol. Inorg. Chem.* **1998**, *3*, 196−200.

(12) (a) Winkler, J. R.; Gray, H. B. *Chem. Rev.* **1992**, *92*, 369−379. (b) Wasielewski, M. R. *Chem. Rev.* **1992**, *92*, 435−461. (c) Paulson, B.; Pramod, K.; Eaton, P.; Closs, G.; Miller, J. R. *J. Phys. Chem.* **1993**, *97*, 13042−13045.

(13) Davis, W. B.; Svec, W. A.; Ratner, M. A.; Wasielewski, M. R. *Nature* **1998**, *396*, 60−63.

(14) (a) Hall, D. B.; Holmlin, R. E.; Barton, J. K. *Nature* **1996**, *382*, 731−735. (b) Núñez, M. E.; Hall, D. B.; Barton, J. K. *Chem. Biol.* **1999**, *6*, 85−97.

(15) (a) Meggers, E.; Michel-Beyerle, M. E.; Giese, B. *J. Am. Chem. Soc.* **1998**, *120*, 12950−12955. (b) Giese, B.; Wessley, S.; Spormann, M.; Lindemann, U.; Meggers, E.; Michel-Beyerle, M. E. *Angew. Chem., Int. Ed.* **1999**, *38*, 996−99.

(16) (a) Henderson, P. T.; Jones, D.; Hampikian, G.; Kan, Y.; Schuster, G. B. *Proc. Natl. Acad. Sci. U.S.A.* **1999**, *96*, 8353−8358. (b) Ly, D.; Sanii, L.; Schuster, G. B. *J. Am. Chem. Soc.* **1999**, JA991753S.

(17) (a) Brun, A. M.; Harriman, A. *J. Am. Chem. Soc.* **1992**, *114*, 3656−3660. (b) Harriman, A. *Angew. Chem., Int. Ed. Engl.* **1999**, *38*, 945−949.

(18) Meade, T. J.; Kayyem, J. F. *Angew. Chem., Int. Ed. Engl.* **1995**, *34*, 352−354.

(19) Murphy, C. J.; Arkin, M. R.; Jenkins, Y.; Ghatlia, N. D.; Bossmann, S. H.; Turro, N. J.; Barton, J. K. *Science* **1993**, *262*, 1025−1029.

(20) (a) Kelley, S. O.; Barton, J. K. *Chem. Biol.* **1998**, *5*, 413−425. (b) Wan, C.; Fiebig, T.; Kelley, S. O.; Treadway, C. R.; Barton, J. K.; Zewail, A. H. *Proc. Natl. Acad. Sci. U.S.A.* **1999**, *96*, 6014−6019.

(21) (a) Fukui, K.; Tanaka, K. *Angew. Chem., Int. Ed. Engl.* **1998**, *37*, 158−161. (b) Fukui, K.; Tanaka, K.; Fujitsuka, M.; Watanabe, A.; Ito, O. *J. Photochem. Photobiol., B* **1999**, *50*, 18−27.

(22) Kelley, S. O.; Barton, J. K. *Science* **1999**, *283*, 375−381.

(23) (a) Lewis, F. D.; Wu, T.; Zhang, Y.; Letsinger, R. L.; Greenfield, S. R.; Wasielewski, M. R. *Science* **1997**, *277*, 673−676. (b) Lewis, F. D.; Letsinger, R. L. *J. Biol. Inorg. Chem.* **1998**, *3*, 215−221.

are totally nonfluorescent. Selective quenching by G:C, but not A:T, base pairs is consistent with an electron-transfer mechanism in which singlet stilbene serves as an electron acceptor and guanine as an electron donor. Incorporation of a single G:C pair at different positions relative to the stilbene linker permitted investigation of the distance-dependent formation and decay of the stilbene anion radical by means of femtosecond time-resolved transient absorption spectroscopy, thus providing the first rate constants for distance-dependent charge separation and recombination in duplex DNA.[23] Rate constants for charge separation calculated from fluorescence intensity and lifetime data were in reasonable agreement with the directly measured values. A more limited data set for charge recombination provided a similar β value. These results are consistent with a superexchange mechanism for electron transfer (eq 1), providing a value of $\beta \approx 0.6$ Å^{-1} for charge separation. The stilbenedicarboxamide-linked hairpins remain the only system for which the decay of the excited-state electron acceptor and the formation and decay of the radical ion intermediates at variable fixed D−A distances in duplex DNA have been directly observed.[23]

We report here the results of our detailed investigation of charge separation and recombination in two families of stilbenedicarboxamide-linked synthetic hairpins possessing a single G:C base pair by means of steady-state fluorescence and femtosecond and nanosecond transient absorption spectroscopy. In the absence of electron transfer, the stilbene linker has a fluorescence quantum yield of 0.38 and decay time of 2.0 ns. These values are exceptionally long for a stilbene and reflect a hairpin geometry which inhibits nonradiative decay via photoisomerization. Analysis of the transient absorption spectra shows that the initially formed stilbene Franck−Condon singlet state undergoes dual exponential relaxation on ca. 10 and 60 ps time scales prior to the 2 ns decay in the absence of competing electron transfer. Electron transfer can be either faster or slower than singlet relaxation depending on the distance between the guanine donor and singlet stilbene acceptor. The two hairpin families differ in that the guanine electron donor is located in the polyT arm in one family and in the polyA arm of the other. Both charge separation and charge recombination rate constants are similar for the two hairpin families, slightly faster rates being observed at short distances when guanine is in the polyA arm. The effects of a second G:C base pair on the dynamics of electron transfer have also been investigated. The presence of adjacent guanines in the same arm results in an increase in the rate constant for charge separation but a decrease in the rate constant for charge recombination when compared to hairpins with a single G:C base pair. These changes are rather modest, suggesting that the GG step is a rather shallow "hole trap". The results of this investigation serve to further elucidate the structure and distance dependence of photoinduced electron transfer via a superexchange mechanism in duplex DNA.

Results

Conjugate Structure and Electronic Absorption Spectra. The preparation of di(hydroxypropyl)amide, DPS, and di(anilinopropyl)amide, DAS, via the reaction of the diacid chloride of *trans*-stilbene-4,4′-dicarboxylic acid with excess amine has been previously described.[26] Prior to incorporation of the diol DPS into a synthetic (bis)oligonucleotide conjugate, it was converted to the monoprotected, monoactivated diol by sequential reaction with 4,4′-dimethoxytrityl chloride and with 2-cyanoethyl diisopropylchlorophosphoramidite. The conjugates shown in Chart 1 were prepared by means of conventional phosphoramidite chemistry using a Millipore Expedite oligonucleotide synthesizer following the procedure developed by Letsinger and Wu.[26] The conjugates were first isolated as tritylon derivatives by RP HPLC, then detritylated in 80% acetic acid for 30 min, and then repurified by RP HPLC. A single peak was detected by both RP and IE HPLC. Molecular weights of the conjugates were determined by electrospray ionization mass spectroscopy.

The identifying symbols for the conjugates in Chart 1 have a number to indicate the position of the G:C base pair(s) relative to the stilbene linker. For the sake of clarity the numbering system has been changed from that used in our earlier publication.[23] The designation *n*G:C is used for conjugates in which G is in the polyT arm and C in the polyA arm, whereas the designation nC:G is used for conjugates in which G is in the polyA arm. Conjugates containing two G:C base pairs have identifying symbols for both base pairs. The hairpin lacking a G:C base pair is designated T_6−A_6.

The ultraviolet absorption spectra of the diol DPS and the conjugate 5G:C are shown in Figure 1a. The long-wavelength band in both spectra is assigned to the fully allowed stilbene π,π^* transition. This band is red-shifted by ca. 8 nm in the conjugate vs DPS. The shorter wavelength 260 nm band in 5G:C is attributed to overlapping absorption bands of the nucleobases and stilbene. All of the conjugates in Chart 1 have absorption spectra essentially identical to that of 5G:C. The absorption spectrum of DAS at wavelengths longer than 300 nm is similar to that of DPS.

Heating of the conjugates in aqueous solution (ca. 5×10^{-6} M conjugate, 0.1 M NaCl, 10 mM Tris−HCl, pH 7) results in a decrease in absorbance (ca. 30% hypochromism) for the 260 nm band. The derivative of the thermal dissociation profile for T_6−A_6 provides a melting temperature $T_M = 59°$ C which is independent of conjugate concentration, supporting the assignment of a hairpin vs duplex structure or aggregate. This value is significantly higher than that expected for a duplex formed between two self-complementary T_6−A_6 conjugates which would possess two duplexes regions, each containing six base pairs, separated by the stilbene linkers (T_M(calcd) = 30 °C[27]). The 330 nm absorbance of T_6−A_6 decreases continuously with increasing temperature. Approximately half of the 7% decrease observed between 0 and 80 °C can be attributed to thermal expansion of water. The remaining hypochromism and the red shift in the absorption maximum relative to DPS might reflect either weak electronic interaction with the adjacent base pair or simply a change in solvation. The conjugate 5G:C has a higher melting temperature, 75 °C, than does T_6−A_6, as expected for the addition of a G:C base pair. The T_M values for hairpins containing two G:C base pairs are too high (>85 °C) to be measured in 0.1 M NaCl. The CD spectrum of the conjugate T_6−A_6 has a positive band at 283 nm and a negative band at 250 nm. Its appearance is similar to that of a polyT−polyA duplex which is known to adopt a B-form double helical structure.[28]

Molecular modeling of T_6−A_6 and the other conjugates in Chart 1 indicates that they can adopt energy-minimized B-form

(24) (a) Lewis, F. D.; Zhang, Y.; Liu, X.; Xu, N.; Letsinger, R. L. *J. Phys. Chem. B* **1999**, *103*, 2570−2578. (b) Lewis, F. D.; Helvoigt, S. A.; Letsinger, R. L. *Chem. Commun.* **1999**, 327−328. (c) Lewis, F. D.; Liu, X.; Miller, S. E.; Wasielewski, M. R. *J. Am. Chem. Soc.* **1999**, *121*, 9746−9747.

(25) Lewis, F. D.; Liu, X.; Wu, Y.; Miller, S. E.; Wasielewski, M. R.; Letsinger, R. L.; Sanishvili, R.; Joachimiak, A.; Tereshko, V.; Egli, M. *J. Am. Chem. Soc.* **1999**, *121*, 9905−9906.

(26) Letsinger, R. L.; Wu, T. *J. Am. Chem. Soc.* **1995**, *117*, 7323−7328.

(27) SantaLucia, J., Jr. *Proc. Natl. Acad. Sci. U.S.A.* **1998**, *95*, 1460−1465.

Chart 1

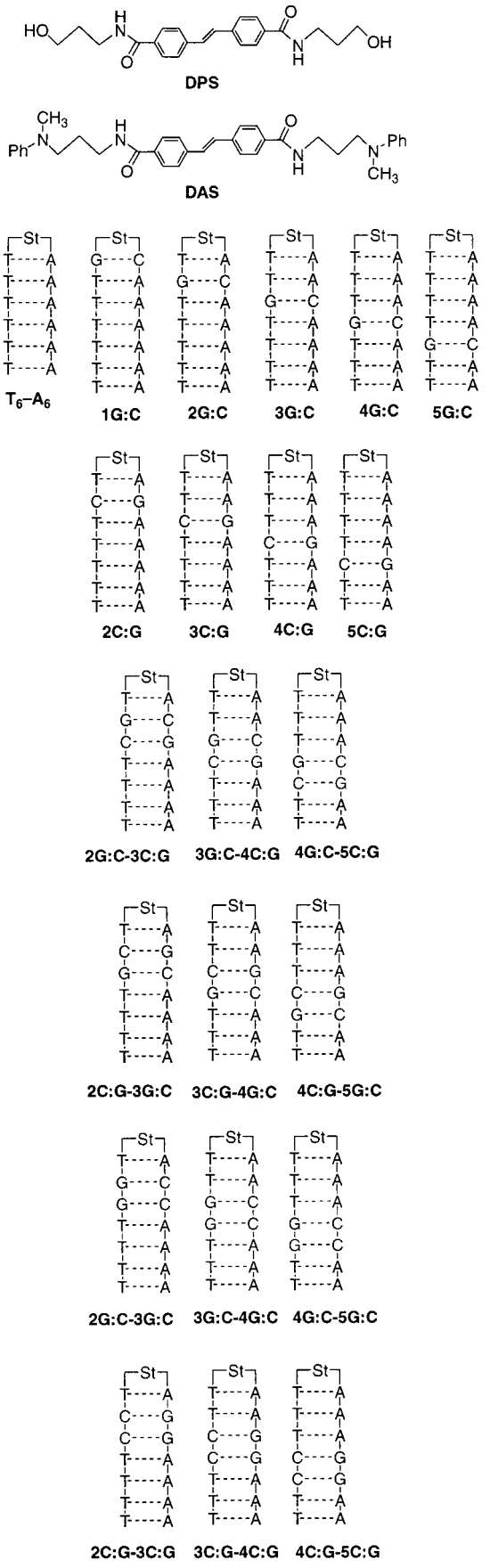

conformations in which the stilbenediamide is approximately coplanar with the adjacent base pair.[29] The minimized structure for 1G:C shown in Figure 2 has a stilbene−guanine plane-to-plane separation of 4.4 Å, somewhat longer that the average base-stacking distance of 3.4 Å in B-form DNA.[30] The hairpins in Chart 1 all possess two or more T:A base pairs at the end of

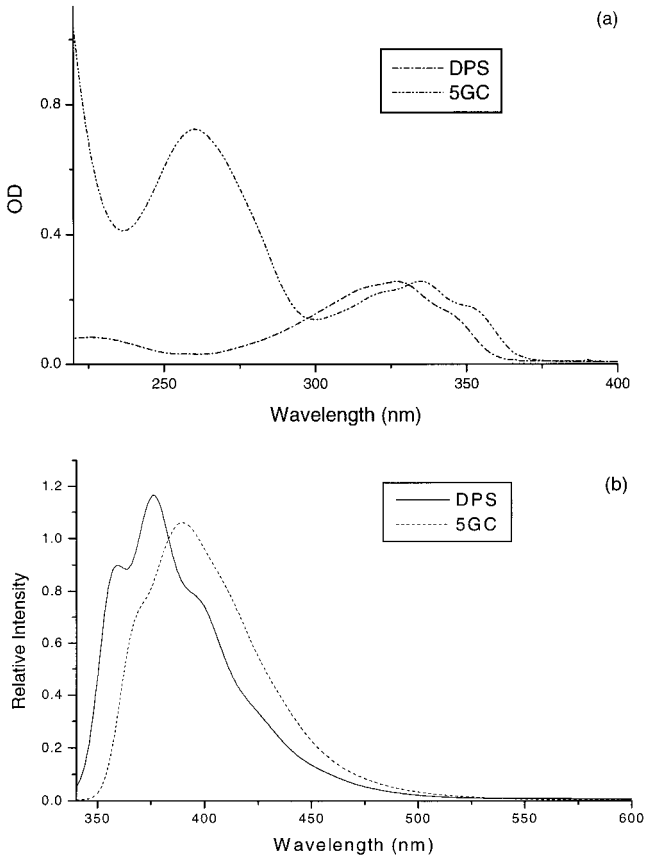

Figure 1. (a) Absorption and (b) fluorescence spectra of the diol DPS in methanol solution (7.7×10^{-6} M) and hairpin 5G:C in aqueous solution (4.9×10^{-6} M, 0.1 M NaCl, 10 mM sodium phosphate, pH 7.2).

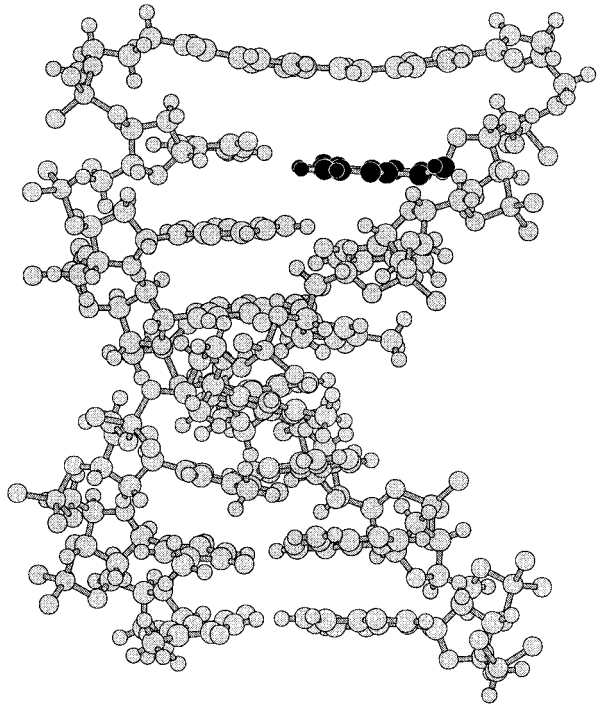

Figure 2. MM2-minimized structure for the hairpin 1G:C. The stilbene linker is shown at the top of the structure, and the guanine is shown with solid atoms.

Table 1. Fluorescence Quantum Yields and Decay Times for Stilbenedicarboxamide Model Compounds and Hairpins[a]

compound	Φ_f[b]	τ_s, ns[c]	compound	Φ_f[b]	τ_s, ns[c]
DPS	0.11[d]	0.28[d]			
DAS	$<10^{-3}$				
T_6-A_6	0.38[e]	1.96			
2G:C	0.040[e]	<0.1	2C:G	0.018	<0.1
3G:C	0.14[e]	0.5	3C:G	0.050	0.3
4G:C	0.26[e]	1.0	4C:G	0.20	0.6
5G:C	0.35[e]	1.5	5C:G	0.35	
2G:C−3C:G	0.038		2C:G−3G:C	0.022	
3G:C−4C:G	0.11		3C:G−4G:C	0.058	
4G:C−5C:G	0.26		4C:G−5G:C	0.16	
2G:C−3G:C	0.035		2C:G−3C:G	0.024	
3G:C−4G:C	0.14		3C:G−4C:G	0.053	
4G:C−5G:C	0.25		4C:G−5C:G	0.16	

[a] Quantum yields and decay times for 5×10^{-6} M model compounds and hairpins determined in deoxygenated 0.1 M aqueous buffer containing 0.1 M NaCl solution except as noted. [b] Quantum yields obtained using phenanthrene as a reference standard ($\Phi_f = 0.13$ in cyclohexane[59]). [c] Fluorescence decay times. [d] Data for methanol solution. [e] Data from ref 23.

the hairpin remote from the stilbene linker. Thus, partial end fraying should not affect π-stacking in the portion of the hairpin containing the stilbene, guanine, and intervening T:A base pairs.

Conjugate Fluorescence. The diol DPS displays weakly structured fluorescence with a maximum at 386 nm in aqueous solution (Figure 1b). Its fluorescence quantum yield and decay time in methanol solution are reported in Table 1. These values are somewhat larger than those for *trans*-stilbene in alkane solution ($\Phi_f = 0.04$, $\tau_s = 70$ ps).[31] The fluorescence rate constant for DPS, calculated from the quantum yield and lifetime ($k_f = \Phi_f \tau_S^{-1}$), is 3.9×10^8 s^{-1}, somewhat smaller than the value for *trans*-stilbene, 5.7×10^8 s^{-1}.[31]

The fluorescence spectrum of 5G:C is red-shifted by 12 nm with respect to that of the diol DPS (Figure 1b). Similar fluorescence spectra are observed for all of the other conjugates, except 1G:C, which is nonfluorescent. Complementary bis(oligonucleotide)−stilbenedicarboxamide conjugates which form stable duplexes display both excimer fluorescence and induced circular dichroism.[32] The absence of such spectral changes for T_6-A_6 and the other conjugates in Chart 1 provides additional evidence for hairpin vs duplex formation.

The fluorescence quantum yields for the conjugates are summarized in Table 1. Within a hairpin family, the fluorescence quantum yield increases with increasing separation between the G:C base pairs and the stilbene linker. Comparison of quantum yield data for the *n*G:C vs *n*C:G families shows that the former have larger values of Φ_f, except in the case of 5G:C and 5C:G, which have the same value. Comparison of the *n*G:C or *n*C:G families with the families having two G:C base pairs either in the same or opposite strands shows that the presence of a second base pair further away from the stilbene linker has little or no effect on the value of Φ_f.

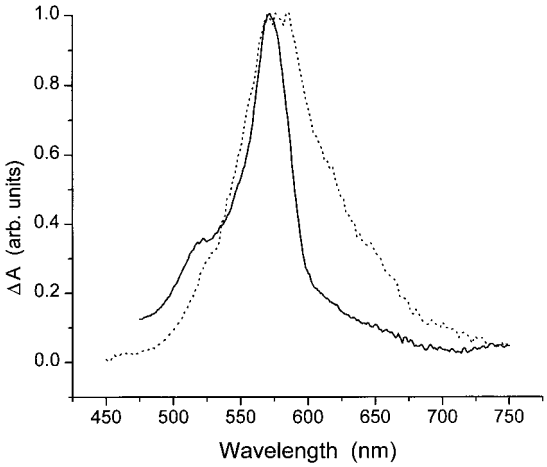

Figure 3. Normalized transient absorption spectra obtained at short delay times following 340 nm excitation. DPS after 2 ps (dashed line) and DAS after 10 ps (solid line).

Fluorescence decays for T_6-A_6 and 3G:C−5G:C have been determined with a fluorescence lifetime apparatus capable of resolving fluorescence decay times of >0.1 ns. All of the decays are best fit by a single-exponential function. The values of τ_S in Table 1 are similar to those previously reported and increase with increasing distance between the G:C pair and stilbene linker.[23] The value of τ_S for T_6-A_6 is substantially longer than that for DPS or *trans*-stilbene. Evidently, the hairpin geometry inhibits torsion about the stilbene double bond, which is responsible for the short singlet lifetimes of DPS and *trans*-stilbene.[33] The calculated values of the fluorescence rate constant for T_6-A_6 and 3G:C−5G:C ($k_f = (2.5 \pm 0.5) \times 10^8$ s^{-1}) are somewhat smaller than the value for DPS ($k_f = 3.9 \times 10^8$ s^{-1}), plausibly reflecting a difference in solvation or perturbation of the stilbene chromophore by the adjacent TA base pair.

Transient Absorption Spectra of the Stilbene Singlet and Anion Radical. The transient absorption spectra of DPS, DAS, and the conjugates were measured with a femtosecond amplified Ti:sapphire-based laser system that has been described previously.[34] A ca. 200 fs, 340 nm laser pulse is used to excite the samples, and a white light probe pulse of somewhat shorter duration is used to monitor the spectra as a function of time. The transient absorption spectrum of the diol DPS obtained at a delay time of 2 ps after excitation is shown in Figure 3. Both the band shape and absorption maximum (570 nm) are similar to those reported by Hochstrasser and co-workers[35] for *trans*-stilbene in hexane solution (585 nm). The molar absorbance of the stilbene $S_1 \rightarrow S_n$ transition is even larger than that of the $S_o \rightarrow S_1$ transition (70 000 vs 28 000),[36] facilitating its detection by transient absorption spectroscopy. The band shape of the DPS transient absorption spectrum obtained at delay times of 5 and 25 ps is superimposable on that obtained at 2 ps.

The transient absorption of singlet DPS in methanol solution reaches its maximum intensity within the time of the excitation pulse (ca. 200 fs). The decay of the DPS transient absorption monitored at 565 nm is monoexponential with a decay time of

(28) (a) Jin, R.; Gaffney, B. L.; Wang, C.; Jones, R. A.; Breslauer, K. J. *Proc. Natl. Acad. Sci. U.S.A.* **1992**, *89*, 8832−8836. (b) Lu, M. Guo, Q.; Kallenbach, N. R. *Biochemistry* **1993**, *32*, 598−601.

(29) Hairpin structures were calculated using the molecular mechanics force field (MM^+) within Hyperchem V5.01a (Hypercube, Waterloo, Ontario). Local minima were optimized assuming normal B-form DNA geometries.

(30) Sriram, M.; Wang, H.-J. In *Bioorganic Chemistry: Nucleic Acids*; Hecht, S. M., Ed.; Oxford; New York, 1996; pp 105−143.

(31) (a) Saltiel, J.; Waller, A. S.; Sears, D. F. Jr.; Garrett. C. Z. *J. Phys. Chem.* **1993**, *97*, 2516−2522. (b) Waldeck, D. H. *Chem. Rev.* **1991**, *91*, 1, 415−436.

(32) Lewis, F. D.; Wu, T.; Burch, E. L.; Bassani, D. M.; Yang, J.-S.; Schneider, S.; Jäger, W.; Letsinger, R. L. *J. Am. Chem. Soc.* **1995**, *117*, 8785−8792.

(33) The quantum yields for photoisomerization of T_6-A_6 and 1G:C in aqueous buffer are 0.042 ± 0.004 and <0.001, substantially smaller than the value of 0.52 for *trans*-stilbene.[28] X. Liu, unpublished results.

(34) (a) Greenfield, S. R.; Wasielewski, M. R. *Opt. Lett.* **1995**, *20*, 1394−1396. (b) Greenfield, S. R.: Svec, W. A.; Gosztola, D.; Wasielewski, M. R. *J. Am. Chem. Soc.* **1996**, *118*, 6767−6777.

(35) (a) Greene, B. I.; Hochstrasser, R. M.; Weisman, R. B. *Chem. Phys. Lett.* **1979**, *62*, 427−430. (b) Hochstrasser, R. M. *Pure Appl. Chem.* **1980**, *52*, 2683−2691.

(36) Yoshihara, K.; Namiki, A.; Sumitani, M.; Nakashima, N. *J. Chem. Phys.* **1979**, *71*, 2892−2895.

220 ps. The stilbenediamide chromophore does not fluoresce at 565 nm (Figure 1b), and thus only the transient absorption is monitored at this wavelength. The 220 ps decay time is somewhat shorter than the 280 ps fluorescence decay time in ethanol−water solution at 23 °C. The latter value is temperature-dependent, increasing to 390 ps at 2 °C.[32] Thus, a difference in either solvent or temperature could account for the small difference in DPS lifetimes obtained by transient absorption and fluorescence decay. The DPS singlet decay time is somewhat longer than that for *trans*-stilbene (110 ps) reported by Hochstrasser et al.,[35] as is the case for the fluorescence decay times.

The bis(anilino)stilbenedicarboxamide DAS was selected as a precursor of the stilbenedicarboxamide anion radical, on the basis of the known ability of tertiary amines to quench stilbene singlets by an electron-transfer mechanism.[37] The energetics of intramolecular electron transfer from a *N*,*N*-dialkylaniline to stilbenedicarboxamide can be estimated using Weller's equation (eq 3), where *C* is the solvent-dependent Coulombic attraction

$$\Delta G_{et} = E_{ox} - E_{red} - E_S + C \qquad (3)$$

energy, which can be neglected in polar solvents such as dimethyl sulfoxide or water.[39] The sum of the singlet energy (3.4 V) and reduction potential (−1.9 V vs SCE in dimethyl sulfoxide solution) for *N*,*N*-dimethylstilbene-4,4′-dicarboxamide is 1.5 V, substantially larger than the oxidation potential of *N*,*N*-dimethylaniline (+0.78 V vs SCE). Thus, electron transfer should be exergonic by ca. 0.7 V.

The transient absorption spectrum of DAS in THF solution obtained at a delay time of 10 ps is also shown in Figure 3. The band shape does not change with delay time (5−100 ps). The band maximum is at 565 nm similar to that of the DPS singlet-state absorption. However, the absorption band of DAS is narrower and possesses a high-energy shoulder at 525 nm which is not present in the spectrum of the DPS singlet. The DAS band shape is similar to that for the *trans*-stilbene anion radical, and thus, both the main band and shoulder are assigned to the DAS anion radical.[39] The cation radical of *N*,*N*-dimethylaniline has an absorption band at 475 nm; however, its molar absorbance is much smaller than that of stilbene (4000 vs 70 000).[39] Thus, the absence of an aniline band in the transient spectrum of DAS is not surprising. The band maximum for the DAS anion radical is at longer wavelength than that for the stilbene anion radical (565 nm for DAS in THF vs 485 nm in 1,2-dichloroethane solution). The electron-withdrawing amide substituents in DAS most likely alter the spacing of state energies and thus decrease the $D \rightarrow D_n$ transition energy of the anion radical.

The transient decay of DAS monitored at 565 nm can be best fit by a double exponential with decay times of 2.2 and 770 ps. The fast decay is assigned to conversion of the stilbene singlet to its anion radical, the charge separation process. The appearance of the transient absorption spectrum (Figure 3) indicates that this process is essentially complete within 5 ps. Very rapid charge separation is consistent with the absence of stilbene fluorescence from DAS. The longer decay time can be attributed to the charge recombination process, which returns the ion pair to the ground state. The rate constants for DAS charge separation and charge recombination are similar to those reported by Mataga et al.[40] for the anthracene−linker−aniline system *p*-$(CH_3)_2$N−Ph−$(CH_2)_3$−(9-anthryl) in polar solvents. Since charge separation is very rapid in these systems, it most likely occurs via a through-bond mechanism that does not require folding of the trimethylene linker prior to electron transfer. Charge recombination is relatively slow due to the large energy gap between the ion pair state and ground state (ca. 2.7 eV in the case of DAS), which should place it deep in the Marcus inverted region.[41] DAS is insoluble in ethanol or ethanol−water solvent. Both its transient absorption spectra and electron-transfer dynamics might be different in aqueous solution vs THF.

Table 2. Transient Decay Times for Stilbenedicarboxamide Model Compounds and Hairpins[a]

compound	τ_r, ps (%)[b,c]	τ_s, ps (%)[c,d]	τ_a, ns (%)[c,e]
DPS		220 (100)	
DAS		2.2 (26)	0.77 (74)
T_6−A_6	6.7 (15), 60 (24)	2,000 (61)[f]	
1G:C		1.0 (26)[f]	0.026 (72)[f]
2G:C		5.1 (17)[f]	0.14 (83)[f]
3G:C	9.2 (26)	120 (23)[f]	3.8 (51)
4G:C	10 (24), 61 (26)	990 (50)[f]	240[g]
5G:C	8.0 (13), 54 (24)	1,400 (52)[f]	*h* (10)
2C:G		3.9 (23)	0.094 (73)
3C:G	6.9 (14)	31 (25)	1.9 (61)
4C:G	12 (22), 40 (17)	460 (24)	57 (36)[g]
5C:G	8.4 (20), 63 (25)	1,400 (41)	*h* (14)
3G:C−4C:G	11 (34)	137 (18)	4.2 (48)
3C:G−4G:C	7.8 (24)	47 (24)	2.0 (52)
2G:C−3G:C		3.4 (39)[i]	0.46 (35)
3G:C−4G:C	7.4 (25)	58 (26)[i]	11.6 (47)
3C:G−4C:G		18 (35)[i]	5.7 (45)[g]

[a] Data for deoxygenated solutions of 2×10^{-5} M model compounds (DPA in methanol and DAS in THF) or hairpins (aqueous buffer containing 0.1 M NaCl). [b] Singlet relaxation occurs without a change in band shape. [c] Percent of the total decay amplitude. Decays longer than 5 ns not included for *n*GC series but included for other hairpins. [d] Singlet decay occurs without a change in band shape for DPS, with a minor change in band shape for T_6−A_6, and with formation of the anion radical in all other cases via charge separation. [e] Decay time of the anion radical. [f] Data from ref 23. [g] Decay time measured by nanosecond laser flash photolysis. [h] Long-lived transient lifetime (>5 ns) not measured. [i] Additional unassigned components (61 ps, 26% for 2G:C−3G:C, 810 ps, 11% for 3G:C−4G:C and 380 ps, 20% for 3C:G−4C:G).

Transient Absorption of the Hairpins T_6−A_6 and 1G:C. The transient absorption spectra of T_6−A_6 and 1G:C obtained at delay times of 10 and 2 ps, respectively, were previously reported.[23a] On the basis of comparisons of their band shapes with those for DPS and DAS (Figure 3), the spectrum of T_6−A_6 was assigned to the stilbene singlet, whereas the spectrum of 1G:C was assigned to the stilbene anion radical. The transient absorption spectra obtained at longer delay times display only minor changes in band shape (see the Supporting Information).

The transient decay curve for T_6−A_6 (see the Supporting Information) is best fit by a triple exponential with decay times of 6.7, 60, and 2000 ps having amplitudes of 15%, 24%, and 61%, respectively (Table 2). The long-lived component has the same decay time as the fluorescence decay (Table 1) and thus is assigned to the decay of the relaxed fluorescent singlet state. The two short-lived components are assigned to the relaxation process of the initially formed Franck−Condon singlet state. The basis for this assignment is provided in the Discussion. The absence of a change in the transient absorption band shape precludes electron transfer as a mechanism for the fast decay processes.

(37) Lewis, F. D.; Bassani, D. M.; Burch, E. L.; Cohen, B. E.; Engelman, J. A.; Reddy, G. D.; Schneider, S.; Jaeger, W.; Gedeck, P.; Gahr, M. *J. Am. Chem. Soc.* **1995**, *117*, 660−669.

(38) Weller, A. *Zeit. Phys. Chem. Neu. Folg.* **1982**, *133*, 93−98.

(39) Shida, T. *Electronic Absorption Sepctra of Radical Ions*; Elsevier: Amsterdam, 1988.

(40) Mataga, N.; Nishikawa, S.; Asahi, T.; Okada, T. *J. Phys. Chem.* **1990**, *94*, 1443−1447.

(41) Marcus, R. A. *J. Chem. Phys.* **1956**, *24*, 966−978.

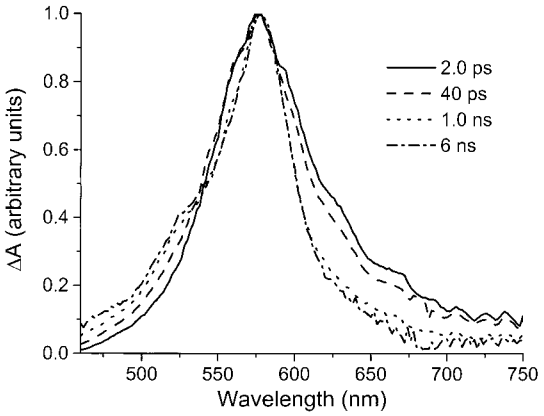

Figure 4. Normalized transient absorption spectra of 3G:C obtained at several delay times following 340 nm excitation.

The transient decay of 1G:C (see the Supporting Information) can be fit by a double exponential with decay times of 1.0 and 26 ps having amplitudes of 26% and 74%, respectively. These are assigned to the formation and decay, respectively, of the stilbene anion radical (Table 2). Ultrafast singlet decay is consistent with the absence of fluorescence from 1G:C. The relatively small decrease in signal amplitude accompanying the fast decay process requires similar values for the molar absorbance of the singlet and anion radical. As previously noted, the singlet and anion radical of *trans*-stilbene are both reported to have a molar absorbance of 70 000.[36,39] The transient absorption spectrum of the guanine cation radical is reported to be broad and weak in the visible region with a molar absorbance of 2000 at 450 nm.[42] Thus, it is not surprising that only the stilbene anion radical is observed in the transient absorption spectrum of 1G:C.

Transient Absorption Spectra of Other *n*G:C and *n*C:G Hairpins. The transient absorption spectra of the hairpins 2G:C−5G:C and 2C:G−5G:C display a time-dependent change in band shape from that of the stilbene singlet to that of the stilbene anion radical. These changes can be clearly seen in the normalized spectra of 3G:C (Figure 4). The picosecond transient decays of 2G:C and 2C:G monitored at 575 nm can be fit to a double exponential with short (ca. 5 ps) and long (ca. 100 ps) components. As in the case of 1G:C the two decays are assigned to the stilbene singlet and anion radical, respectively (Table 2). Both decays are slower than those for 1G:C. Rapid singlet decay is consistent with the observation of very weak fluorescence with a decay time of <100 ps (Table 1).

The decays of 3G:C and 3C:G are more complex, requiring triple-exponential fits. The short-lived component is assigned to relaxation of the Franck−Condon singlet, on the basis of the absence of a change in band shape during its decay and a decay time similar to that for the short-lived component of T_6-A_6 (Table 2). The second component is assigned to formation of the anion radical from the relaxed singlet stilbene. It is accompanied by a change in band shape and, in the case of 3G:C, has a decay time similar to that of the fluorescence decay (Table 1). The long-lived component has a band shape similar to that of DAS and is assigned to the anion radical.

The hairpins 4G:C, 5G:C, 4C:G, and 5C:G have decays which require quadruple exponential fits. The two shorter-lived components have decay times of 7−12 and 40−60 ps for both hairpins, similar to those for T_6-A_6, and are assigned to relaxation of the Franck−Condon singlet state (Table 2). The third components are assigned to formation of the anion radical from the relaxed singlet. They are accompanied by a change in band shape similar to that shown in Figure 4 and have nanosecond decay times which, in the case of 4G:C and 5G:C, are similar to the fluorescence decay times (Table 1). The fourth components are assigned to decay of the stilbene anion radical, on the basis of their band shape and decay times, which are much longer than the 2 ns decay of T_6-A_6. They are too long-lived for measurement with the ps apparatus. In the case of 4G:C and 4C:G the decay of the anion radical was determined using a nanosecond apparatus (Figure 5, inset). The transient spectrum decays completely to the baseline with decay times of 240 and 57 ns, respectively, for 4G:C and 4C:G.

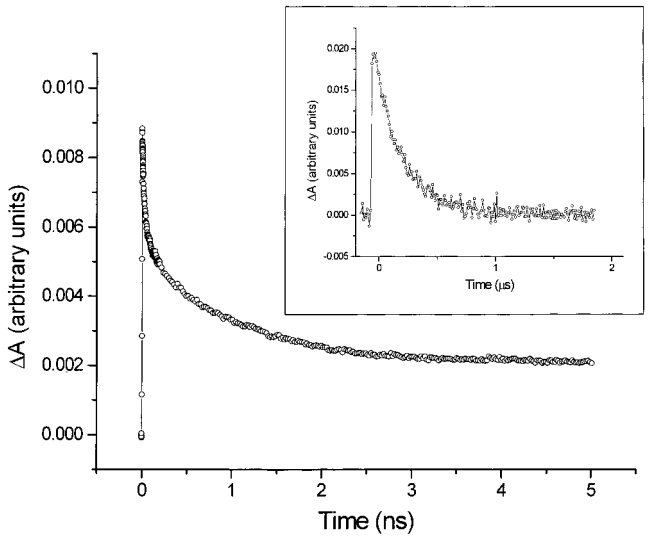

Figure 5. Transient decay of 4G:C monitored at 575 nm on nanosecond and microsecond (inset) time scales.

Decay times for the Franck−Condon singlet state, relaxed singlet state, and anion radical are summarized in Table 2. Both the charge separation and charge recombination decay times for the *n*C:G hairpin family are shorter than those for the *n*G:C family, except in the case of 5C:G and 5G:C, which have similar values. Additional support for the assignments in Table 2 is provided by changes in amplitude observed when the decays are monitored at longer and shorter wavelengths (625 and 525 nm, respectively). The amplitudes of the decay components assigned to the Franck−Condon and relaxed singlet states increase at 625 nm, whereas the amplitudes of the long-lived components assigned to the anion radical increase at 525 nm. The decay times and amplitudes reported in Table 2 are obtained from a single transient decay curve, but are representative of results obtained for multiple measurements on the same and different samples of a given conjugate. It should be noted that the triple and quadruple exponential fits obtained for these hairpins are not merely a case of distributed kinetics. Correlation of decay times with changes in the transient absorption band shape and independently measured fluorescence decay times permits their assignment with a high level of confidence.

Electron Transfer in Hairpins Containing Two G:C Base Pairs. The appearance of the transient absorption spectra of hairpins containing two G:C base pairs is similar to that of hairpins containing a single G:C base pair. Spectra of 3C:G-4C:G are shown in Figure 6. Analysis of the transient decays yields the decay times summarized in Table 2. In the case of the hairpins 3G:C−4C:G and 3C:G−4G:C, which have guanines in opposite strands, the decay times assigned to relaxation of the Franck−Condon state, conversion of the relaxed singlet to

(42) Candeias, L. P.; Steenken, S. *J. Am. Chem. Soc.* **1989**, *111*, 1, 1094−1099.

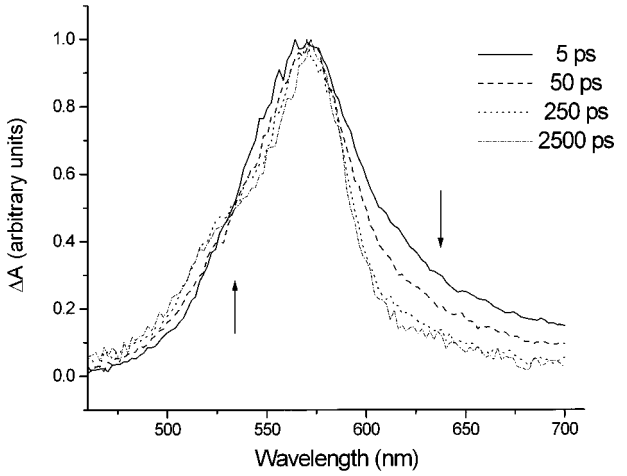

Figure 6. Normalized transient absorption spectra of 3C:G-4C:G obtained at several delay times following 340 nm excitation.

the anion radical, and decay of the anion radical are all similar to those for the hairpins 3G:C and 3C:G, respectively. Thus, the presence of a second 4G:C or 4C:G base pair has little effect on the dynamics of charge separation and charge recombination when the guanines are in opposite strands.

The hairpins 2G:C−3G:C, 3G:C−4G:C, and 3C:G−4C:G, which have guanines in the same strand, display more complex kinetics for singlet-state decay. The assignments of decay components reported in Table 2 are consistent with changes in the time-dependent transient absorption spectra (Figure 6). However, for each of these hairpins there is an additional component of intermediate decay time that remains unassigned and might result from either a second slow charge separation process or a fast charge recombination process. It is important to note that the change in dynamics for the hairpins containing a GG step is not reflected in their fluorescence quantum yields, which are similar to those for hairpin families with a single G:C base pair or two G:C base pairs with guanine in opposite strands (Table 1).

Discussion

The stilbene-linked DNA hairpins possess structures which make them uniquely well-suited for investigations of photoinduced electron transfer in duplex DNA. The location of the stilbene chromophore with respect to the duplex formed by the two arms of the bis(oligonucleotide) is unambiguously defined, with the stilbene located adjacent to the base pair formed by the nearest-neighbor 3′ and 5′ bases. The CD spectrum of the hairpin T_6-A_6 and high melting temperatures for all of the hairpins are indicative of a B-form duplex structure for the base-paired hairpin stem. We have recently reported the crystal structure of a stilbene diether-linked hairpin with a base sequence similar to that of 1G:C.[25] The unit cell contains four stilbene-linked hairpins, all of which possess B-form structures with the stilbene diether parallel to an adjacent G:C base pair, with an average plane-to-plane separation of 3.25 Å, slightly shorter than the average base-stacking distance in DNA.[30] The four hairpins in the unit cell have highly similar π-stacking geometries, but differ in their sugar−phosphate backbone conformations. Molecular modeling of 1G:C (Figure 2) indicates that it can adopt a B-form structure with the stilbenediamide chromophore approximately parallel to the adjacent G:C base pair. The calculated (gas-phase) stilbene−guanine plane-to-plane distance, 4.4 Å, is larger than that for the stilbene diether; however, hydrophobic interactions may lead to a reduction in this distance in solution. The use of the natural nucleobase guanine as the electron donor ensures that the hairpin structure is not disrupted by the donor.

The photophysical behavior of stilbenediamide linker makes it well-suited for the investigation of photoinduced electron transfer. The stilbene ground state, singlet state, and anion radical all have large molar absorbances,[36,39] facilitating their study in the highly dilute solutions needed to avoid aggregation of oligonucleotides. The absorption and fluorescence band shapes of 5G:C in aqueous solution are similar to those for the diol DPS in methanol solution (Figure 1); the small red shifts can be attributed to the difference in the environment of the chromophore. The long-wavelength absorption band displays weak hyperchromism and no induced circular dichroism. Similar small perturbations of the electronic spectra have been observed for related hairpin structures[24,25] and for end-stacked aromatic hydrocarbons.[43] The fluorescence quantum yield and lifetime of the stilbenediamide in T_6-A_6 are longer than those of either the diol DPS (Table 1) or unsubstituted *trans*-stilbene; however, its radiative rate constant is similar to those of DPS and stilbene. Inhibition of the usual stilbene singlet-state nonradiative decay pathway, torsion about the central double bond, can account for the long lifetime, high fluorescence quantum yield, and low photoisomerization quantum yield of T_6-A_6.[33] The relatively high fluorescence quantum yield for T_6-A_6 and 3G:C, 4G:C, and 5G:C (Table 1) ensures that the results of fluorescence quenching studies are representative of a significant fraction of the excited hairpins. In addition, the observation of single-exponential nanosecond fluorescence decay for these hairpins indicates that either the fluorescent hairpins are structurally homogeneous on the nanosecond time scale or that hairpins with different sugar−phosphate backbone conformations have the same decay time.

The driving force for photoinduced charge separation and charge recombination in the stilbene-linked hairpins can, in principle, be calculated using Weller's equation (eq 3). However, the oxidation potentials of the nucleobases have not been measured in duplex DNA. Values have been measured for the nucleobases and deoxynucleosides in both aqueous and non-hydroxylic polar solvents.[44] Significantly lower oxidation potentials for all four nucleosides are reported in aqueous vs nonaqueous solution. This difference is attributed to the occurrence of coupled electron and proton transfer in aqueous solution. We have proposed that the use of nonaqueous potentials is appropriate for studies of rapid, reversible electron transfer in duplex DNA because of the hydrophobic environment of the nucleobases.[24a] Using the oxidation potentials for dG and dA reported by Seidel et al.[44c] (1.22 and 1.69 V, respectively), calculated values of ΔG_{et} are ca. −0.3 eV for dG and +0.2 for dA, as shown in Figure 7. These values are consistent with the observation of rapid photoinduced electron-transfer quenching of singlet stilbene by dG in 1G:C but not by dA in T_6-A_6.

The calculated driving force for charge separation in 1G:C is smaller than that for DAS (−0.3 vs −0.7 eV), yet the singlet decay time of 1G:C is more rapid (Table 2). The decay time for the anion radical is also shorter for 1G:C than for DAS, even though the calculated ion pair energy is larger for 1G:C. This seeming anomaly may reflect differences in either the

(43) Ren, R. X.-F.; Chaudhuri, N. C.; Paris, P. L.; Rumney, S.; Kool, E. T. *J. Am. Chem. Soc.* **1996**, *118*, 7671−7678.

(44) (a) Steenken, S.; Telo, J. P.; Novais, H. M.; Candeias, L. P. *J. Am. Chem. Soc.* **1992**, *114*, 4701−4709. (b) Shafirovich, V. Y.; Courtney, S. H.; Ya, N.; Geacintov, N. E. *J. Am. Chem. Soc.* **1995**, *117*, 4920−4929. (c) Seidel, C. A. M.; Schulz, A.; Sauer, M. H. M. *J. Phys. Chem.* **1996**, *100*, 5541−5553.

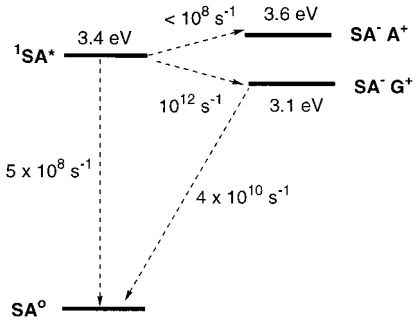

Figure 7. Energetics and dynamics of charge separation and charge recombination from singlet stilbeneamide (SA) to an adjacent adenine (A) in T_6-A_6 or guanine (G) in 1G:C.

solvent polarity (water vs THF) or the electron-transfer pathway. D−B−A systems with flexible linkers are believed to adopt extended conformations in polar solvents. In contrast, the hairpin ion pair may adjust its local structure by contracting the D−A distance and by increasing the overlap between the radical ions and between the guanine cation radical and adjacent bases. Computational evidence for stabilization of nucleobase cation radicals by interactions with adjacent bases has been provided by Sugiyama and Saito[45] and Prat et al.,[46] and Schuster[16] has suggested that a nucleobase cation radical in DNA is delocalized over several adjacent bases.

Assignment of Transient Decay Components. The assignment of the individual decay components to the transient absorption spectra is crucial to the interpretation of the dynamics of charge separation and charge recombination in our hairpin systems. The stilbene singlet model compound DPS undergoes single-exponential decay with no change in band shape. This is consistent with the report of Hochstrasser and co-workers[35] that the band shape of singlet *trans*-stilbene does not change following excitation at 308 nm. Their earlier observation that time-dependent band narrowing occurs within the 50 ps following 265 nm excitation presumably is due to relaxation of the vibrationally excited singlet state.[35a] The hairpin T_6-A_6 undergoes triple-exponential decay, but no change in the band shape of the transient absorption spectrum. The long-lived 2.0 ns transient decay has the same decay time as that obtained from the nanosecond fluorescence decay (Table 1) and thus is assigned to decay of the relaxed stilbene singlet state (τ_s).

For the hairpins containing a single G:C base pair, the decay component with the second longest lifetime is assigned to the charge separation process ($\tau_s = \tau_{cs}$), which results in conversion of the relaxed stilbene singlet to the anion radical. This assignment is supported by a change in the transient absorption band shape from that of the singlet-state model DPS to that of the anion radical model DAS (compare Figures 3 and 4) on this time scale. In cases where fluorescence decay times have been directly measured (Table 1), they are in reasonable agreement with the transient decay times (Table 2). For all hairpins containing G:C base pairs, the longest-lived decay process is assigned to the charge recombination process. Essentially complete decay of the transient absorption signal occurs on time scales ranging from 26 ps for 1G:C to 240 ns to 4G:C (Table 2). Since degradation of the stilbene long-wavelength absorption band occurs slowly under both steady-state and pulsed laser excitation, anion radical decay is assumed to occur predominantly via charge recombination with the guanine cation radical.

In the case of T_6-A_6 and several of the hairpins containing G:C base pairs, transient decay components with decay times of ca. 10 and 60 ps are observed that are not associated with a change in the transient absorption band shape. These decay components are assigned to relaxation processes of the initially formed Franck−Condon singlet state. Whereas Hochstrasser et al.[35] observed no change in the transient absorption band shape following 308 nm excitation of *trans*-stilbene, Iwata and Hamaguchi[47a] have reported that changes in the bandwidth and peak positions of the C=C and C−phenyl Raman stretching modes occur on the picosecond time scale following 294 nm excitation in heptane solution. Narrowing of the bandwidth occurs within ca. 10 ps, whereas the change in peak position occurs over a period of 40 ps. These changes were attributed to rapid vibrational cooling followed by slower structural changes which accompany solvent relaxation. Relaxation is thought to yield a singlet excited state which is more planar than the ground state. Similar biphasic decay on the picosecond time scale has been observed for singlet stilbene by Schultz et al.[47b] by means of time-resolved anti-Stokes Raman scattering in hexane and methanol solution. Evidently, the stilbene transient absorption spectrum is not sensitive to the processes that are observed by transient Raman spectroscopy.

Decay of the two short-lived components for T_6-A_6 occurs on the same time scales as the relaxation processes observed for singlet stilbene by transient Raman spectroscopy.[47] However, as noted above, the transient absorption spectrum of DPS does not change on this time scale. Thus, the fast relaxation pathways for T_6-A_6 most likely involve geometric relaxation of the chromophore and duplex. Increased planarity of the stilbene chromophore upon relaxation of the Franck−Condon singlet state would permit a more effective π-stacking with the adjacent TA base pair. This could result in a decrease in absorption intensity without a change in band shape, analogous to the hypochromism observed for ground-state π-stacked aromatic chromophores.[48] In support of this possibility, we observe stronger ground-state electronic interaction with the planar diphenylacetylene-4,4′-dicarboxamide hairpin linker than with the nonplanar stilbenedicarboxamide linker.[24c,49] The slower 60 ps relaxation pathway may involve motion of the DNA hairpin, which would permit increased π-orbital overlap of the stilbene singlet with the adjacent base pair.

Experimental and theoretical studies indicate that the duplex sugar−phosphate backbone undergoes conformational changes on a time scale of 20−200 ps, but that base pair hydrogen bonds remain intact on this time scale.[50] A recent investigation of the dynamic Stokes shift of a duplex containing a fluorescent base pair analogue found the interior of DNA undergoes geometry changes on slower time scales (300 ps and 13 ns).[51] Our hairpin crystal structure also displays much larger variation in the conformation of the sugar−phosphate backbone than in the π-stacking of the base pairs.[25]

Distance-Dependent Charge Separation and Charge Re-

(45) Sugiyama, H.; Saito, I. *J. Am. Chem. Soc.* **1996**, *118*, 7063−7068.
(46) Prat, F.; Houk, K. N.; Foote, C. S. *J. Am. Chem. Soc.* **1998**, *120*, 0, 845−846.
(47) (a) Iwata, K.; Hamaguchi, H. *Chem. Phys. Lett.* **1992**, *196*, 462−468. (b) Schultz, S. L.; Qian, J.; Jean, J. M. *J. Phys. Chem. A* **1997**, *101*, 1000−1006.
(48) Cantor, C. R.; Schimmel, R. R. *Biophysical Chemistry*; W. H. Freeman: San Francisco, 1980; pp 399−404.
(49) The crystal structures of the *N,N*-dimethylarene-4,4′-dicarboxamides of stilbene and diphenylacetylene have nonplanar and planar chromophores, respectively. Lewis, F. D.; Yang, J.-S.; Stern, C. L. *J. Am. Chem. Soc.* **1996**, *118*, 12029−12037.
(50) (a) Nordlund, T. M.; Andersson, S.; Nilsson, L.; Rigler, R.; Gräslund, A.; McLaughlin, L. W. *Biochemistry* **1989**, *28*, 9095−9103. (b) Georghiou, S.; Bradrick, T. D.; Philipetis, A.; Beechem, J. M. *Biophys. J.* **1996**, *70*, 1909−1922. (c) Kojima, C.; Ono, A.; Kainosho, M.; James, T. L. *J. Magn. Reson.* **1998**, *135*, 310−333.

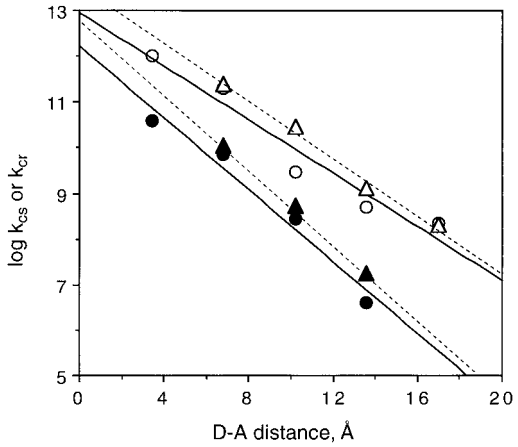

Figure 8. Distance dependence of the rate constants obtained from transient absorption data for charge separation (open symbols) and charge recombination (filled symbols) from *n*G:C (○, ●, solid lines) and nC:G (△,▲, broken lines) hairpin families.

Table 3. β Values for Charge Separation and Charge Recombination[a]

hairpin family	data set (no. of points)	β, Å^{-1}	k_o, s^{-1}
*n*G:C, charge separation	transient absorption (5)	0.66	7.9×10^{12}
*n*C:G, charge separation	transient absorption (4)	0.71	3.2×10^{13}
*n*G:C, charge recombination	transient absorption (4)	0.90	1.6×10^{12}
*n*C:G, charge recombination	transient absorption (3)	0.94	6.3×10^{12}

[a] Obtained from the slopes of the plots shown in Figures 8.

combination. Rate constants for charge separation can be calculated from the singlet decay times of the *n*G:C and *n*C:G hairpins, τ_n, and the T_6-A_6 hairpin, τ_0 ($k_{cs} = \tau_s^{-1} - \tau_0^{-1}$). Plots of log k_{cs} vs the plane-to-plane stilbene−guanine distance, calculated assuming an average 3.5 Å base-stacking distance, for the *n*G:C and *n*C:G hairpins are shown in Figure 8. Values of k_{cs} decrease from 1×10^{12} s^{-1} for 1G:C to 2×10^8 s^{-1} for 5G:C or 5C:G. Measurements of k_{cs} at larger stilbene−guanine distances are precluded by the short lifetime of the stilbene singlet (Table 1). In the case of 5G:C and 5G:C the values of k_{cr} are smaller than the rate constant for decay of singlet T_6-A_6. According to eq 1, the slopes and intercepts of the plots in Figure 8 provide the values of β and k_o, respectively, which are summarized in Table 3. In the case of 1G:C there is no TA base pair separating the donor and acceptor, and thus it is not formally a D−B−A system. However, deletion of the 1G:C data points has little effect on the calculated values of β for the *n*G:C hairpin family.

Values of β can also be obtained from plots of the fluorescence lifetime data and from the fluorescence quantum yield data (Table 1) according to eq 4, where Φ° is the quantum

$$k_{cs} = \tau_0^{-1}(\Phi^\circ/\Phi_n - 1) \qquad (4)$$

yield for T_6-A_6 and Φ_n is the quantum yield for *n*G:C or *n*C:G. The values of β obtained from the fluorescence lifetime and quantum yield data (0.4−0.5 Å^{-1}; see the Supporting Information) are smaller than the values obtained from the transient absorption data for singlet decay. These differences are somewhat larger than the estimated experimental error of ±0.1 Å^{-1}. There are several possible sources of the disagreement between the values of β obtained from transient absorption and fluorescence data. The fluorescence decay times for 1G:C and 2G:C are too short to measure, and that for 3G:C is near the time resolution of our instrumentation. Similarly, the fluorescence quantum yields for both 1G:C and 2G:C are quite small, whereas that for 5G:C is nearly as large as that for T_6-A_6. The same is true of the fluorescence data for the *n*C:G hairpin family (Table 1). In addition, the fluorescence data provide information only for the subset of hairpins which are fluorescent, which excludes 1G:C completely and is <10% of the singlet states in the case of 2G:C, 2C:G, and 3C:G. It is for these hairpins that the difference in calculated values of k_{cs} obtained from fluorescence and transient absorption data is largest. Thus, we would caution against the use of fluorescence quantum yield data to determine the distance dependence of photoinduced electron transfer, particularly in cases where the quantum yields are small or show no correlation with transient absorption data.

The stilbene anion radical in all of the *n*G:C and *n*C:G hairpins decays by a single-exponential process. Thus, rate constants for charge recombination can be calculated directly from the anion radical lifetimes ($k_{cr} = \tau_a^{-1}$), which can be assigned unambiguously from the transient decays. Plots of log k_{cr} vs the plane-to-plane stilbene guanine distance are shown in Figure 8 and the resulting values of β and k_o reported in Table 3. The values of β for charge recombination are somewhat larger than those for charge separation, as previously observed by Brun and Harriman[17a] in their study of the dynamics of electron transfer between intercalated donors and acceptors. The larger value of β and smaller value of k_o for charge recombination vs charge separation can be attributed to the highly exergonic nature of the former process, which places it within the Marcus "inverted region".[41]

As a consequence of the larger value of β for charge recombination vs charge separation, the ratio k_{cs}/k_{cr} increases with increasing D−A separation. Thus, increasing the D−A separation results in a decrease in the quantum yield of charge separation but an increase in the lifetime of the charge-separated species. This could have important consequences for the efficiency of processes such as hole hopping and oxidative strand cleavage, which must compete with charge recombination. For example, if the first-order rate constant for the initial chemical reaction leading to strand cleavage were 10^6 s^{-1}, the hairpin 4G:C would undergo ca. 6% cleavage whereas the hairpin 2G:C would undergo <1% cleavage, despite the much larger quantum yield of charge separation for the latter hairpin.

The values of β for both charge separation and charge recombination are slightly larger for the *n*C:G hairpin family vs the *n*C:G hairpin family (Table 3). This is a consequence of larger rate constants for short D−A separations ($n < 5$) for the *n*G:C family but similar rates at long D−A separations ($n = 5$). Thus, the kinetic advantage for electron transfer via a polypurine vs polypyrimidine strand appears to be rather small and to operate only over short distances. The dynamics of electron transfer might also be dependent upon hairpin polarity. However, we have prepared analogues of 2G:C and 3G:C with reversed 3′−5′ polarity and find that they have the same fluorescence quantum yields and decay times as those for members of the *n*G:C family.[52]

Comparisons with Theory and Experiment. The *n*G:C and *n*C:G hairpin families can be viewed as donor−bridge−acceptor (D−B−A) systems in which the singlet stilbene functions as an electron acceptor (or hole donor), a variable number of TA base pairs functions as the bridge, and the nucleobase guanine serves as the electron donor (hole acceptor). Our hairpin system has been analyzed by Jortner et al.,[10] who suggest that charge separation occurs via a single-step superexchange mechanism

(51) Brauns, E. B.; Madaras, M. L.; Coleman, R. S.; Mruphy, C. J.; Berg, M. A. *J. Am. Chem. Soc.* **1999**, *121*, 11644−11649.

(52) J. Liu, unpublished results.

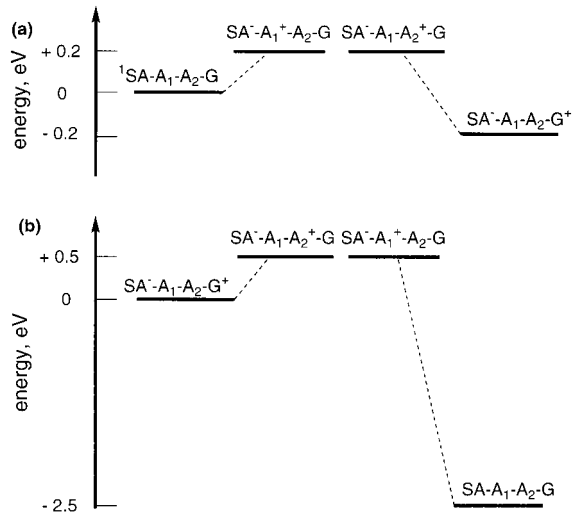

Figure 9. Energetics of (a) charge separation and (b) charge recombination in the stilbene-linked hairpins 3G:C or 3C:G which have two TA base pairs separating the stilbeneamide (SA) acceptor and guanine (G) donor (after Jortner et al.[10]).

in which singlet stilbene serves as a hole donor and guanine as a hole acceptor. The simplest theoretical models for electron transfer via a superexchange mechanism predict an exponential decrease in rate constant with D−A separation (eq 1), in accord with our experimental results for both charge separation and charge recombination (Figure 8).

A state energy level diagram for both the charge separation and charge recombination process in the stilbene-linked hairpins is shown in Figure 9 for a hairpin with two A:T bridging sites (3G:C or 3C:G). The virtual states $S^-A_1{}^+A_2G$ and $S^-A_1A_2{}^+G$ lie above $^1S^*$ by ca. 0.2 eV and thus presumably are not thermally populated in the charge separation process (Figure 9a), in accord with the absence of charge separation in T_6-A_6. In the charge recombination process (Figure 9b), the virtual states lie ca. 0.5 eV above the ion pair state and charge recombination is highly exergonic. Thus, the slower rate constants for charge recombination vs charge separation (Figure 8) may result from either weaker coupling of the initial state with the bridge or the highly exergonic nature of the charge recombination process, which presumably places it in the Marcus inverted region.[41]

Beratan et al.[11b] have calculated the distance dependence of electron transfer in several DNA model systems, including the end-tethered duplex studied by Meade and Kayyem,[18] the nontethered intercalators studied by Brun and Harriman,[17a] and the tethered intecalators studied by Barton et al.[19] In all three cases, the calculated value of β lies in the range 1.2−1.6 Å^{-1}, similar to the values reported for electron transfer via σ-bonded bridges.[13] Values of $\beta \approx 1.4$ Å^{-1} were also calculated for π-stacks of several aromatic hydrocarbons.[11d] In a recent commentary, Beratan et al.[11d] suggest that the smaller value of β observed for our hairpin systems might result from the close proximity of the stilbene HOMO to the DNA HOMOs. Experimental evidence that optimized energy matching between the excited donor and bridge can result in molecular-wire-like behavior in a non-DNA D−B−A system has recently been reported by Wasielewski et al.[13] To our knowledge, such optimization has not been achieved in a DNA D−B−A system.

The observation of similar values of β for the *n*G:C vs *n*C:G hairpin families (Table 3) is somewhat surprising. Jortner et al.[10] predicted that virtual states involving T should lie at much higher energy than those involving A and thus should make only a small contribution to the electron-transfer rate. Stronger coupling might also be expected for polyA vs polyT strands as a consequence of more extensive orbital overlap for purine−purine vs pyrimidine−pyrimidine steps.[30] However, Beratan and co-workers[11] calculated similar couplings along the polyT vs polyA strands of a Meade−Kayyem duplex and similar β values for stacks of benzenes vs naphthalenes. It is, of course, possible that electron transfer in the *n*G:C hairpin family occurs via the polyA strand with cross-strand coupling to guanine. Electron transfer is known to occur efficiently across hydrogen-bonded interfaces, and thus strand-to-strand electron or hole transfer could presumably occur at any base pair within a duplex bridge.[53] However, Risser et al.[11a] report significantly larger intra- vs interstrand coupling. Risser et al.[11a] also predict that the drop off in rate should be "somewhat anisotropic", giving rise to "hot and cold spots". The value of k_{cs} for 3G:C (Figure 8) may represent a "cold spot".

Alternative mechanisms for long-distance electron transfer in D−B−A systems have been advanced by several groups. Friesner et al.[54] predicted on the basis of their solution to the Redfield equation for the density matrix of the full D−B−A system that an activated distance-independent adiabatic mechanism might become significant under highly specific conditions. Davis et al.[55] developed a similar model using a phenomenological treatment of the interaction of a quantum mechanical system with an external bath. According to Friesner,[52] the adiabatic pathway can result in rate constants faster than those for the distance-dependent superexchange mechanism studied by Jortner,[10] Beratan,[11] and their co-workers under certain well-defined conditions. Among these is the requirement of thermal population of the bridge states which can occur only when the D−B gap is very small and the temperature is moderately high. Even under these conditions, the adiabatic mechanism may be slower than superexchange when the bridge contains only a small number of sites,[54] as is the case for our hairpin systems.

Following our initial report of distance-dependent electron transfer in the *n*G:C hairpin family, several other research groups have reported β values for electron hole transfer from guanine or a more readily oxidized nucleobase analogue to an acceptor via a variable number of TA base pairs. Tanaka and co-workers[21] employed an acridine dye which is covalently attached to the sugar−phosphate backbone of a nucleotide and forms a duplex with a complementary strand, in which an acridine acceptor occupies the space of a base pair. The acridine steady-state fluorescence is totally quenched by an adjacent G:C base pair, but the fluorescence quenching decreases when TA base pairs separate acridine and the G:C base pair. Using values of k_{cs} calculated from fluorescence lifetime data, values of $\beta = 1.5$ Å^{-1} and $k_o = 1.9 \times 10^{12}$ s^{-1} were obtained. A large A−B energy gap could account for both the smaller value of k_o and the larger value of β when compared to our stilbene-linked hairpins.

Giese and co-workers[15a] have investigated the distance dependence of hole transport in DNA by site-selective photochemical generation of a guanine cation radical and determining the efficiency of its transfer to a GGG hole trap via a variable number of A:T base pairs. On the basis of relative yields of strand scission, which are assumed to be proportional to the

(53) (a) Sessler, J. L.; Wang, B.; Harriman, A. *J. Am. Chem. Soc.* **1995**, *117*, 704−714. (b) Roberts, J. A.; Kirby, J. P.; Nocera, D. G. *J. Am. Chem. Soc.* **1995**, *117*, 8051−8052.

(54) Felts, A. K.; Pollard, W. T.; Friesner, R. A. *J. Phys. Chem.* **1996**, *99*, 2929−2940.

(55) Davis, W. B.; Wasielewski, M. R.; Ratner, M. A.; Mujica, V.; Nitzan, A. *J. Phys. Chem. A* **1997**, *101*, 6158−6164.

relative rates of electron transfer, a value of $\beta = 0.7$ Å^{-1} was obtained. These workers conclude that four adjacent A:T base pairs effectively block hole transport, but that hole hopping can occur in competition with chemical reactions of the initially formed guanine cation radical when only one or two A:T base pairs separate G:C pairs.

Barton and co-workers have investigated distance-dependent electron transfer in DNA using a number of different donors and acceptors.[7a] Most closely comparable to our results is the recent study by Kelly and Barton[22] of quenching of the fluorescent base analogues 1-N^6-ethanoadenine (A_ϵ) and 2-aminopurine (A_2) by guanine or the more readily oxidized 7-deazaguanine. Quenching of singlet A_ϵ by an adjacent guanine is relatively slow ($k_q \approx 10^9$ s^{-1} from fluorescence lifetime measurements), and the distance dependence of the relative fluorescence intensity or fluorescence decay times provides a value of $\beta = 1.0$ Å^{-1}. These results are similar to those obtained by Fukui and Tanaka[17] and may reflect poor electronic coupling between A_ϵ, which is too bulky to fit into the B-form DNA structure, and the adjacent base pair. Different results were obtained for A_2, which forms a stable base pair with T and can thus be incorporated into duplex structure with normal base-stacking distances. In this system, only static quenching was observed and the values of k_{cs} were assumed to be too fast to measure ($>10^{10}$ s^{-1}). Analysis of the intra- and interstrand quenching of the A_2 fluorescence intensity provided values of the distance dependence of electron transfer in the range 0.1−0.6 Å^{-1}.

Barton and co-workers[20] have also reported weakly-distance-dependent electron transfer involving tethered metallointercalators or organic dyes as electron acceptors. Barton and Zewail et al.[20b] have recently reported the results of an investigation of the femtosecond dynamics of a D−B−A system in which a tethered ethidium intercalator (E), a singlet state acceptor, and the nucleobase analogue 7-deazguanine (Z), the electron donor, are separated by a variable number of A:T base pairs. Their E−B−Z system is the only system studied with subpicosecond time resolution since our initial report on the hairpin systems.[23] Since the results obtained by Barton and Zewail[20b] are used to support the DNA molecular wire paradigm, they merit special mention. Modeling studies and measurements of photoinduced damage indicate that intercalation occurs between the two terminal base pairs (ca. 70%) or between the second and third base pairs (ca. 30%). The dynamics of ethidium singlet-state decay were studied by means of transient absorption and fluorescence up-conversion for systems in which the donor Z is located at the fifth, sixth, or seventh base pair. A 1−10 ps decay component is observed both for systems containing Z and those in which it is absent and thus presumably do not undergo electron transfer. A second 75−100 ps component is also observed for the hairpins containing Z. In addition, a significant nanosecond decay component is observed, in accord with the results of a previous study in which dual exponential decays with decay times of ca. 3 and 9 ns were observed in both the presence and absence of Z.[20a] The two picosecond components of the singlet-state decay for the E−B−Z systems are assigned to distance-independent ultrafast electron transfer. However, transient absorption spectra of the products of electron transfer have not been reported. The similarity of these results to those for the singlet-state decay of the stilbene-linked hairpin T_6−A_6, which lacks an electron donor, and the hairpins 4G:C and 5G:C (or 4C:G and 5C:G) is striking. In the absence of species-associated transient absorption spectra, it seems likely to us that the 1−10 ps decay and 75−100 ps decays may correspond to excited-state relaxation processes similar to those discussed for our hairpin systems, rather than electron-transfer processes.

Charge Separation and Recombination Involving GG Steps. Oxidative cleavage of native DNA is known to occur selectively at the 5′-G of 5′-GG-3′ sites.[4,14,16] Selective cleavage is attributed to the ability of a GG step to serve as a hole trap. Calculations by Sugiayam and Saito[45] and Prat et al.[46] indicate that the ionization potential of a base-paired guanine in duplex DNA is sensitive to the identity of the adjacent base(s), GG steps having the lowest oxidation potential. The calculated ionization potential for a duplex GG step is ca. 0.3 eV lower than that of guanine stacked with any other nucleobase.[45]

We have investigated the dynamics of charge separation and charge recombination in several hairpins containing two adjacent G:C base pairs (Table 2). When the guanines are in opposite strands, the dynamics are the same as those for hairpins with a single G:C in the location proximal to the stilbene linker. Thus, the distal G:C has little effect on electron-transfer dynamics. When the two adjacent guanines are in the same strand, the values of k_{cs} are faster than those for hairpins containing a single G:C base pair by a factor of ca. 2. This change is surprisingly small, considering the much larger driving force expected for photoinduced electron transfer using GG vs a single guanine as the electron donor.[45,46] Evidently, coupling of the excited stilbene acceptor with the poly(A:T) bridge (Figure 9a) is more important than the driving force in determining the rate constant for charge separation. Conversely, charge recombination is slower by a factor of ca. 3 for hairpins containing a GG step than for hairpins containing a single G:C base pair. The lower ionization potential for a GG step should result in a smaller energy gap for charge recombination. For processes in the Marcus inverted region, this should result in a larger rate constant, contrary to the experimental result. However, an increase in the energy gap between the ion pair state and bridge states (Figure 9b) could lead to a decrease in rate. It is also possible that relaxation of the GG geometry occurs following cation radical formation, resulting in a shorter π-stacking distance, as is observed for aromatic hydrocarbon dimer cation radicals.[56] This could result in a large reorganization energy for charge recombination and thus a decrease in the rate constant for this process.

The modest increase in k_{cs} and decrease in k_{cr} for a GG step vs an isolated G indicate that the residence time of the electron hole should be longer on GG than G, but that the GG step does not function as a true hole trap. This result is consistent with recent studies of photoinduced DNA strand scission by Schuster[16] and Barton[14] and their co-workers. They find that strand scission in duplex DNA containing several GG steps occurs not only at the GG step closest to the primary electron acceptor, but also at more remote GG steps. Moreover, Schuster et al.[16b] report that a GG step forms a less effective hole trap than does a single 7,8-dihydro-8-oxoguanine.

Concluding Remarks. In summary, the unique structural and spectroscopic properties of the stilbenediamide-linked hairpins have permitted a detailed investigation of the dynamics of charge separation and charge recombination in DNA over relatively short distances (3.5−17.5 Å). Rate constants for both charge separation and charge recombination are found to decrease exponentially with increasing D−A separation, in accord with a single-step superexchange mechanism for electron transfer. The values of β determined by transient absorption spectroscopy

(56) Majima, T.; Tojo, S.; Takamuku, S. *J. Phys. Chem. A* **1997**, *101*, 1048−1055 and references therein.

are ca. 0.7 $Å^{-1}$ for charge separation and 0.9 $Å^{-1}$ for charge recombination (Table 3). These values are smaller than those for D−B−A systems with protein or saturated hydrocarbon bridges, but larger than those for systems with fully conjugated π-bridges. There is no evidence for either wire-like behavior or gated electron transfer in our hairpin systems; however, we cannot exclude the occurrence of such processes with low efficiency (<5%).

Comparison of the results for the *n*G:C vs *n*C:G hairpin families (Chart 1) indicates that both charge separation and charge recombination are slightly more rapid when the guanine donor is located in the polyA vs poly T hairpin arm. However, this is a short-range effect which is not observed for larger D−A separations. Even at short distances, the effect is smaller than might have been expected on the basis of greater π-orbital overlap for polypurines vs polypyrimidines and the lower bridge state energies for A vs T (Figure 9a). It is of course possible that electron transfer in the *n*G:C hairpin family occurs predominately via the polyA strand with G oxidation occurring via interstrand electron transfer. Both theory and experiment suggest that interstrand electron transfer can compete with intrastrand electron transfer in DNA.

At the time of our initial report of the dynamics of electron transfer in DNA,[23] it was difficult to reconcile our results with observations of long-range oxidative cleavage and repair processes in DNA.[7a] Giese and co-workers[15] provided an elegant solution to this dilemma with their report of hole hopping in DNA, the occurrence of oxidative cleavage at sites remote from the original position of hole generation. Related results have been reported by Schuster,[16] Barton,[14] and, most recently, Nakatani et al.[57] Schuster[16] concludes that these long-range processes occur via a hopping mechanism for cation radical migration termed "phonon-assisted polaron hopping", rather than via a delocalized system with wire-like properties. These investigations indicate that long-distance electron transfer can occur in DNA, but do not establish the efficiency (quantum yield) or dynamics of the hole-hopping process. Studies of the dynamics of hole hopping in stilbene-linked hairpins containing multiple G:C base pairs are currently in progress.

Methods for optimization of the yield and lifetime of charge separation have been extensively studied in D−B−A systems, especially in models for the photosynthetic reaction center.[58] Similar principles should apply to DNA charge separation. One approach is to control the driving force for charge separation and recombination. This has been accomplished to some extent by the use of a GG step as an electron acceptor in our hairpin systems. The increase in k_{cs} and decrease in k_{cr} for a GG step (Table 2) should increase the initial yield and prolong the lifetime of the primary GG hole acceptor. When coupled to a secondary hole acceptor, this could result in more effective hole hopping. The use of triplet electron acceptors such as the anthraquinones employed by Schuster and co-workers[16] could also increase the lifetime of the primary triplet radical ion pair for which charge recombination is a spin-forbidden process. Chemical scavenging of the anion radical by oxygen has also been employed by Schuster to prevent charge recombination.[16] Giese and co-workers[15] generate an isolated guanine cation radical via a photochemical cleavage reaction under conditions where charge recombination presumably cannot occur. Thus, efficient long-distance electron transfer may be achieved in DNA without the need for a new paradigm.

Experimental Section

Oligonucleotides. Oligonucleotide−stilbenedicarboxamide conjugates were prepared by means of conventional phosphoramidite chemistry using a Millipore Expedite oligonucleotide synthesizer following the procedure of Letsinger and Wu.[26] 2′-Deoxynucleotide phosphoramidites and 3′ terminal nucleoside controlled pore glass support (CPG) were purchased from Glen Research (Sterling, VA). The conjugates were first treated with concentrated ammonium hydroxide at 55 °C for 8 h, and then isolated as trityl-on derivatives by RP HPLC and detritylated in 80% acetic acid for 30 min. A single peak was detected by both reversed-phase RP and ion exchange IE (pH 12) HPLC. RP HPLC analysis was carried out on a Dionex chromatograph with a Hewlett-Packard Hypersil ODS-5 column (4.6 × 200) and a 1% gradient of acetonitrile in 0.03 M triethylammonium acetate buffer (pH 7.0) with a flow rate of 1.0 mL/min. IE HPLC analysis was carried out using a Dionex chromatograph with a NucleoPac PA-100 (2 × 200) column and a 1% gradient of 10 mM NaOH in 1.0 M NaCl with a flow rate of 1.0 mL/min. Molecular weights were determined by means of electrospray ionization mass spectroscopy with a Micromass Quattro II atmospheric pressure ionization (API) spectrometer. Oligonucleotide conjugates was purified by RP HPLC, and then by a Nensorb 20 Nucleic Acid Purification Cartridge (New Life Science Products, Boston, MA) prior to direct loop injection.

Electronic Spectroscopy. UV spectra were recorded on a Hewlett-Packard 8452A diode array spectrophotometer. Thermal dissociation profiles were determined using a Pekin-Elmer lambda 2 UV spectrophotometer equipped with a temperature programmer for automatically increasing the temperature at the rate of 0.5 °C/min. Circular dichroism spectra were obtained using a JASCO J-175 spectropolarimeter. Fluorescence spectra were measured using a Spex Fluoromax spectrometer equipped with a RM6 Laude circulation bath for temperature control. Fluorescence decay times were measured using a PTI Strobe Master fluorescence lifetime spectrometer equipped with a hydrogen-filled gated arc lamp (fwhm ca. 1.7 ns). The shortest measurable decays are ca. 0.1 ns. Fluorescence quantum yield and decay time measurements for the oligonucleotide conjugates (5×10^{-6} M) were conducted in 10 mM sodium phosphate, pH 7.2 buffer. All samples were deoxygenated by purging with nitrogen. Quantum yields were determined using phenanthrene as a reference standard ($\Phi = 0.13$ in cyclohexane[59]).

Transient Absorption Spectroscopy. The apparatus used for femtosecond transient absorption spectroscopy is described in detail elsewhere.[34] Briefly described, a small percentage (ca. 5%) of the 800 nm output of a regeneratively amplified Ti:sapphire laser (150 ps, 2 kHz, 350 μJ/pulse) is focused with a 100 mm f.1 lens onto a 2 mm thick sapphire disk. A stable white light continuum is generated by adjusting the intensity of the pump beam to slightly above threshold and then split into probe and reference beams. To generate the 340 nm excitation pulse, the output of an optical parametic amplifier tuned to 680 nm was frequency doubled by focusing it with a 200 mm lens onto a 2 mm thick type I LBO. The frequency-doubled light was collimated, and a $\lambda/2$ waveplate was used to set the polarization of the pump beam at the magic angle (54.7°) with respect to the probe beam to avoid anisotropic effects. The pump beam is chopped at half the repetition rate of the laser. Typical pump energies were 100−500 nJ/pulse. The probe beam is focused separately using a 400 mm f.l lens. The probe and reference beams are vertically displaced, collimated, and focused into a computer-controlled monochromator (Spex 270M) with a 75 mm f.1 lens. The two beams are still spatially separated after the exit slit and detected with matched silicon photodiodes. The amplifier outputs were measured with gated integrators and digitized with a 12-bit A/D board within a personal computer. The total instrument function is 200 fs. Each shot pair (pump on, pump off) results in a single ΔA measurement. The reference pulse, in addition to being

(57) Nakatani, K.; Dohno, C.; Saito, I. *J. Am. Chem. Soc.* **1999**, *121*, 10854−10855.

(58) (a) Gust, D.; Moore, T. A.; Moore, A. L. *Acc. Chem. Res.* **1993**, *26*, 198−205. (b) Kurreck, H. Huber, M. *Angew. Chem., Int. Ed. Engl.* **1995**, *34*, 849−866.

(59) Birks, J. B. *Photophysics of Aromatic Molecules*; Wiley-Interscience: London, 1970; p 128.

used for the ΔA calculation, is used to discriminate against probe pulses of abnormal intensity. Data sets are typically the average of 5−10 scans, with each point in the scan being an average of 200 laser shots. Samples have optical densities at 340 nm of 0.10−0.15 in a 2 mm path length cell (concentration $\sim 2 \times 10^{-5}$ M). Samples were stirred using a wire stirrer to prevent thermal lensing and sample degradation. Little or no bleaching of the 340 nm absorption band (<10%) was observed in the femtosecond experiments.

Transients with decay times of >5 ns were determined using a 10 Hz Nd:YAG laser system. The frequency-tripled output of the YAG (355 nm, 5 ns) was used to excite the sample and could be blocked by a computer-controlled shutter. The probe light was generated by a homemade xenon flashlamp with the wavelength selected using an Instruments-SA TRIAX 180 monochromator and detected with a Hammamatsu R298 photomultiplier with only four dynodes wired-up. Typically, 10 laser shots with the pump beam on and pump beam off were averaged by a LeCroy 9384 digital oscilloscope. A computer was used to store the signal and subtract the "data/pump-off" from "data/pump-on" to give one measurement ("gate") of ΔA kinetics. Lifetimes of up to 4 μs can be recorded with this apparatus. Samples of 0.10−0.15 optical density in a 1.0 cm path length cell were purged with nitrogen. Optical degradation was minimized by use of low pump energies (6 mJ/pulse) and a 450 nm long wavelength-pass filter for the probe light. Ten gates (100 pump shots) yielded acceptable signal/noise ratios without significant sample degradation (<20% bleaching of the 340 nm absorption band).

Acknowledgment. This research is supported by funding from the Division of Chemical Sciences, Office of Basic Energy Sciences, U.S. Department of Energy, under Contracts DE-FG02-96ER14684 (F.D.L.) and W-31-109-Eng-38 and DE-FG02-99ER14999 (M.R.W.). We thank Mark Ratner for useful suggestions.

Supporting Information Available: Normalized transient absorption spectra of T_6-A_6 and 1G:C at several decay times, singlet wavelength transient decays of T_6-A_6 and 1G:C, and the distance dependence of the rate constants for charge separation obtained from fluorescence quantum yield data (PDF). This material is available free of charge via the Internet at http://pubs.acs.org.

JA993689K